16th World Conference on Earthquake, 16WCEE 2017

Santiago Chile, January 9th to 13th 2017

Paper N° 808 (Abstract ID)

Registration Code: S-Q1463211555

Evaluation of Elastic Stiffness and Yield Strength of High Strength Steel Square Tube Column to Beam Flange Connections with Exterior Diaphragm

R. Oba(1), T. Kinoshita(2), K. Suita(3), Y. Koetaka(4), S. Matsuo(5), Y. Murakami(6)

(1) *Grad. Student, Dept. of Architecture and Architectural Eng., Kyoto University, oba.ryosuke.m1@gmail.com*
(2) *Senior Researcher, Civil Engineering Dept., Steel Research Lab., JFE Steel Corp., Dr. Eng., to-kinoshita@jfe-steel.co.jp*
(3) *Prof., Dept. of Architecture and Architectural Eng., Kyoto University, Dr. Eng., suita@archi.kyoto-u.ac.jp*
(4) *Assoc. Prof., Dept. of Architecture and Architectural Eng., Kyoto University, Dr. Eng., koetaka@archi.kyoto-u.ac.jp*
(5) *Assoc. Prof., Faculty of Human-Environment Studies, Kyushu University, Dr. Eng., matsuo@arch.kyushu-u.ac.jp*
(6) *Staff Deputy General Manager, Construction Materials & Development Dept., JFE Steel Corp., M. Eng., yu-murakami@jfe-steel.co.jp*

Abstract

In recent years, high strength steels, whose tensile strength is more than 780 MPa, have been developed in Japan, and are used mainly for columns of high rise building structures. However, it is difficult to secure not only quality but also workability of welding at beam-to-column connections with high strength steel. In Japan, most well used shape of columns is a square hollow section but this type of closed cross section is necessary to stiffen the section by a diaphragm at the location of the joint with beam flanges to restrain local deformation. In this study, we focus on exterior diaphragm type connection. Because a diaphragm plate is attached only from outside of a column and columns need not to be cut, this type of diaphragm has advantage to overcome the problem about workability of welding of high strength steels. Furthermore, the exterior diaphragm is suitable for applying concrete filled steel tubes with high strength steels.

For improving convenience of construction and transportation efficiency, this study regards a square diaphragm of thick steel plate, whose depth of protrusion is smaller than a conventional exterior diaphragm. In case of the exterior diaphragm, out-of-plane deformation of steel tube wall occurs. Accordingly, the methods to evaluate elastic stiffness and yield strength of beam-to-column connection are necessary to design the connection. In this study, we focus on tension sides of moment connection where tensile force is transmitted from a beam flange.

To evaluate elastic stiffness and yield strength theoretically, only the beam flange connection is picked up and a mechanical model consisted of two parts, i.e. "exterior diaphragm model" and "column model", is used. The exterior diaphragm model is made of elasto-plastic wire elements having the same mechanical properties as diaphragms, and the column model is made by rigid-body spring model of the column. Then, we consider that elastic stiffness of the beam flange connection occurs under same deformations of two parts, and presume that elastic stiffness of the connection is equal to the sum of stiffness of two parts. We consider yield strength of the beam flange connection as the sum of resistant forces of two parts at the instant when the diaphragm model yields under bending moment and shear force, or axial force, while the column model is still under elastic range.

FEM analysis and loading tests are conducted on beam flange connections, and calculated values of elastic stiffness and yield strength were compared with results of analysis and tests. Investigated parameters are the thickness and the width of columns, width of beam flanges, and the thickness and depth of the projection of diaphragms. The beam flange is subjected to force in one direction, and elastic stiffness and yield strength of beam flange connections were obtained. As a result, it is confirmed that calculated values correspond with results of many analysis and tests well and the validity of the proposed method is confirmed.

Keywords: High Strength Steel, Exterior Diaphragm Moment Connection, Beam to Flange joint, Elastic Stiffness, Yield Strength

1. Introduction

In recent years, high strength steel called as H-SA700, whose tensile strength is more than 780 MPa, has been developed in Japan[1], and is used mainly for columns of high rise building structures. In general, severe construction management and advanced technique of welding with high strength steels are required to secure high quality of welds such as the strength, toughness, and penetration of welded parts[2]. In particular, welding construction at beam to high strength steel column connnections is very important.

In Japan, square hollow section columns are usually used in order to make bi-directional moment resisting frames. This type of closed cross section is necessary to stiffen the section by a diaphragm at the location of the joint with beam flanges to restrain local deformation. Through diaphragms are most generally adapted at beam to column connnections of Japanese steel structures shown in Fig.1(a).

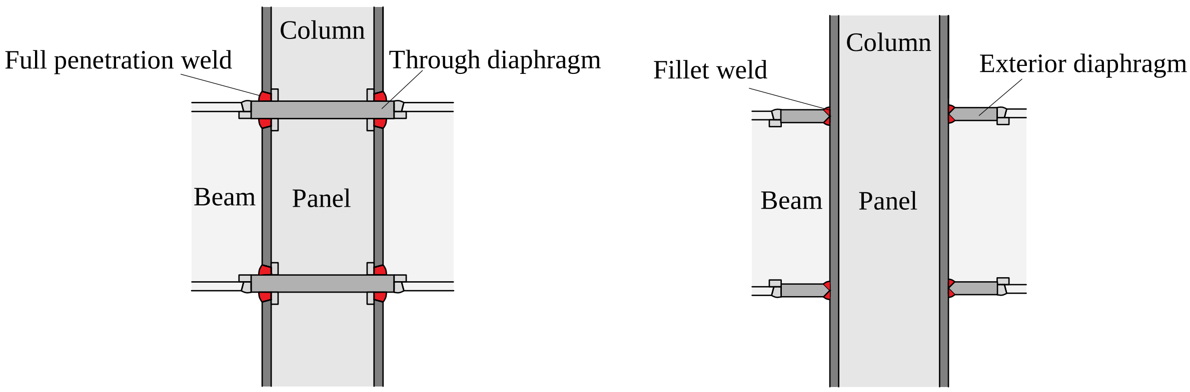

(a)Through diaphragm (b)Exterior diaphragm

Fig.1 Kinds of diaphragm type connections

At the through diaphragm type connection, columns and through diaphragms are connected by full penetration welding, and the strength of diaphragms and welding material must be generally higher than that of columns. However, the strength of welding material for 780MPa class steels are nearly equal to that of 780MPa class steels, and there is a possibility that the strength of welded parts is lower than that of base material, depending on welding conditions. Thereby, severe welding conditions are needed to secure appropriate strength and toughness of welded parts, and it is difficult to adapt through diaphragms at beam to high strength steel column connections in terms of workability of welding. Therefore, in this study, we focus on an exterior diaphragm type connection (Fig.1(b)).

Because the diaphragm plate is attached only from outside of the column at the exterior diaphragm type connection, columns need not to be cut, and diaphragms and welding material whose strength can be equal to that of beams can be generally used. Furthermore, it is possible that CO_2 arc welding is adapted. Therefore, this type of diaphragms has advantage to overcome the problem about workability of welding of high strength steels. For improving convenience of construction and transportation efficiency, this study regards a square diaphragm of thick steel plate (Fig.2), whose depth of protrution is smaller than a conventional exterior diaphragm (Fig.3).

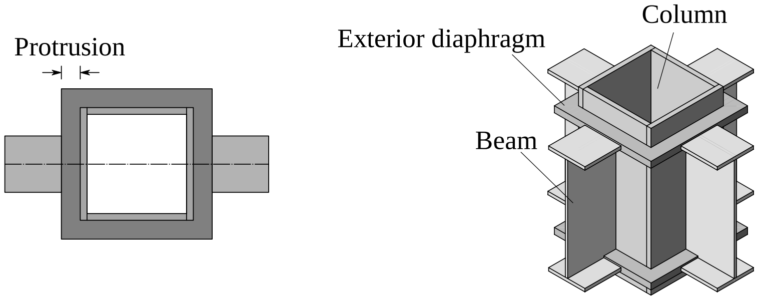

Fig.2 – Small protrusion exterior diaphragm

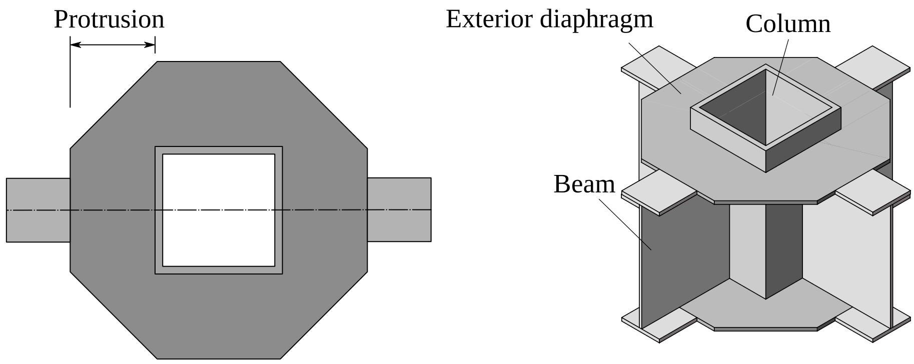

Fig.3 - Conventional exterior diaphragm

When the beam to column connection with exterior diaphragms is subjected to bending moment M, out-of-plane deformation of column shown in Fig.4(a) and in-plane deformation of exterior diaphragm shown in Fig.4(b) generally occur because columns have the hollow section. Thus the stiffness and the strength of exterior diaphragm type connections are lower than those of through diaphragm type connections.

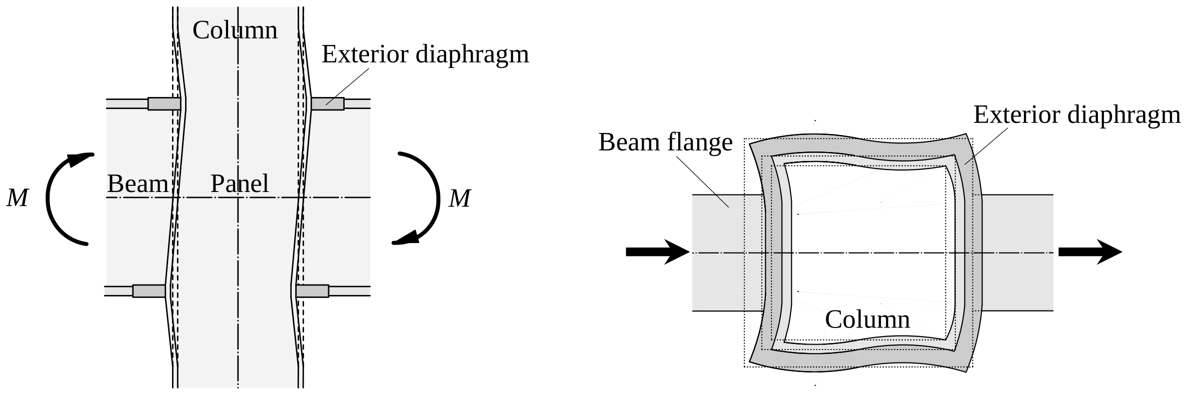

(a)Out-of-plane deformation of column (b)In-plane deformation of exterior diaphragm

Fig.4 – Deformation of column and exterior diaphragm

Accordingly, the methods to evaluate elastic stiffness and yield strength of beam to column connections are necessary to design the connection. Past study about evaluation methods of elastic stiffness has been conducted by Nakamura[3]. However, it has had a problem that out-of-plane deformation of column was not taken into consideration. On the other hand, Ito has proposed the evaluation formula of yield strength, which is given by multiplying plastic strength obtained in plastic analysis simply by 0.85[4]. However, this coefficient 0.85 has been given so that values of calculation are consistent with experimental results, and how widely that evaluation formula has been able to be applied was not clear. Therefore, in this study, proposing evaluation methods of elastic stiffness and yield strength of beam to column connections with the exterior diaphragm is aimed. Furthermore, to verify the validity of evaluation methods, we compared calculated values with results of loading tests and FEM analysis.

2. Calculation of Elastic Stiffness and Yield Strength

2.1 Models for calculation of elastic stiffness

This study regards an interior column shown in Fig.5(a). When the beam to column connection is subjected to bending moment M and stress acting on the beam web is ignored, tesile or compressive force acting on the beam flange is M/d_b, where d_b is the distance between upper and lower plate thickness center of beam flanges. The tensile side is considered in this study, and the area surrounded by a broken line in fig.5(a) is replaced with the local tensile model shown in fig.5(b), in which tensile force P is applied to the beam flange joint. We presume that mechanical behavior of the beam flange joint of the compressive side is consist with that of the tension side, and it is possible to evaluate elastic stiffness and yield strength of the compressive side by the evaluation methods of this study.

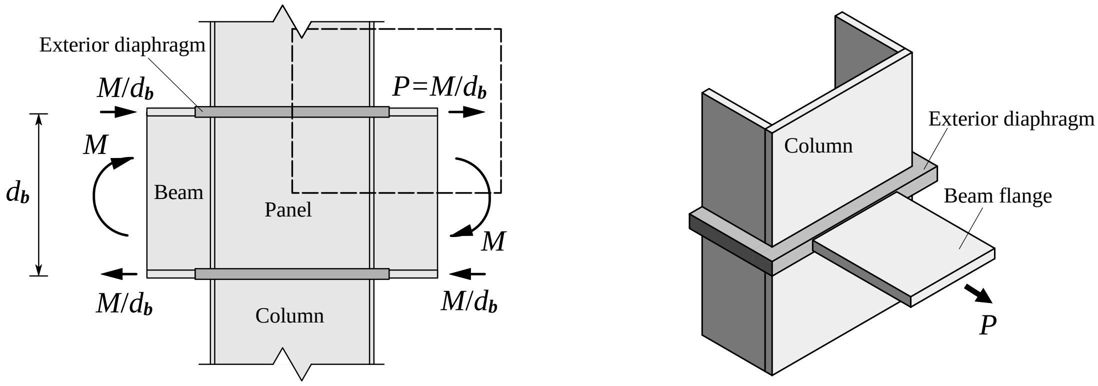

(a)Beam to column connection (b)Local tensile model

Fig.5 – Modeling of beam to column connection

To establish evaluation methods of elastic stiffness and yield strength theoretically, local tensile model is divided to two parts. One part is the exterior diaphragm (see Fig.6 : exterior diaphragm model) and another part is the steel tube wall of the column (see Fig.7 : column model).

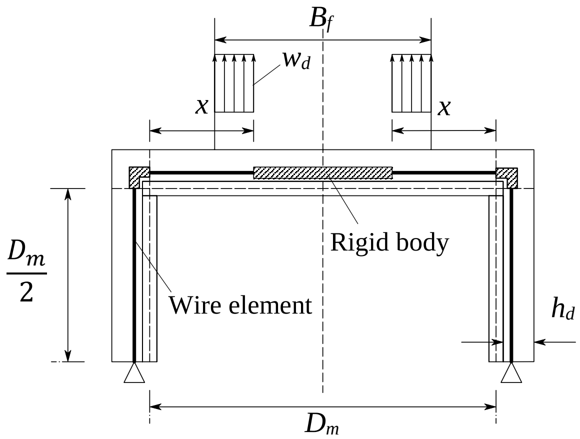

Fig.6 - Exterior diaphragm model

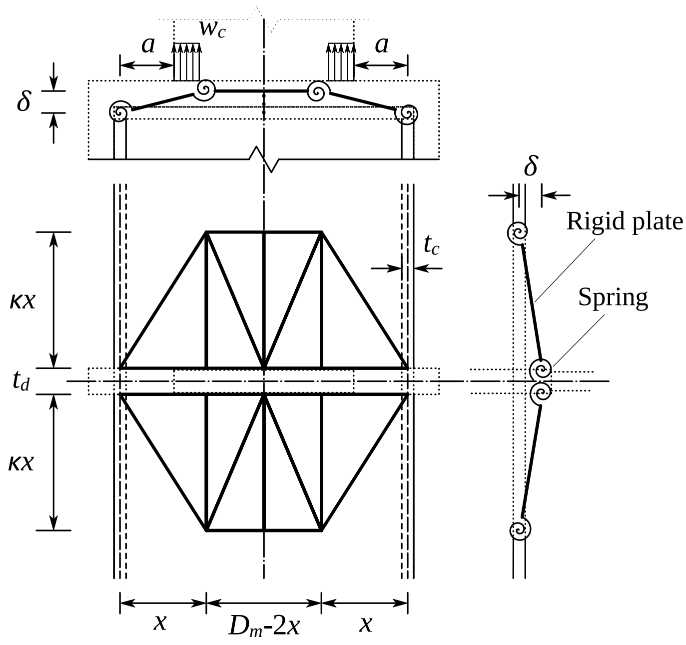

Fig.7 - Column model (by RBSM)

The exterior diaphragm model is made of the exterior diaphragm and steel tube wall of column, whose length of the axial direction of the column is t_d (diaphragm thickness), and these sections is replaced with elasto-plastic wire elements having the rectangular cross section. Rigid bodies are located at the shaded area in Fig.6. Stress from the beam flange is an uniformly distributed load w_d in the exterior diaphragm model, and is w_c in the column model, considering that stress acts on both edges of the beam flange. Elastic stiffness of the exterior diaphragm model K_d is given by considering bending, shearing, and axial deformation of wire elements.

On the other hand, rigid-body spring model[5] (which is called RBSM) is applied to the column model. The steel tube wall of the column is devided into several triangle elements which are treated as rigid-body, and these elements are connected by elastic springs. Elastic stiffness of the column model K_c is given by

$$K_c = \frac{16D_p}{x+a}\left(\frac{D_m}{\kappa^3 x^2} + \frac{\kappa}{x} + \frac{2}{\kappa x} + \frac{2\kappa}{D_m}\right) \tag{1}$$

Where D_m is the distance between two plate thickness center of column flanges, and D_p is flexural rigidity of the plate per unit width. D_p is given by the following equation, where t_c is thickness of the column, E is Young's modulus, and ν is Poisson's ratio,

$$K_c = \frac{Et_c^3}{12(1-\nu^2)} \tag{2}$$

Then, we consider that elastic stiffness of the local tensile model shown in Fig.5(b) occurs under the same deformation of two parts, and presume that elastic stiffness of the tensile model K is equal to the sum of stiffness of two parts. Therefore, K is given by

$$K = K_d + K_c \tag{3}$$

2.2 Calculation formula of x and κ

Strain energy of the beam flange joint W is given by the following equation, where δ is the magnitude of deformation in Fig.7,

$$W = \frac{1}{2}K\delta^2 = \frac{1}{2}(K_d + K_c)\delta^2 \tag{4}$$

Then we consider that κ, which determines the measure of height direction of the column model, is obtained by the condition of minimizing W, or K. Therefore, κ is given by

$$\kappa = \sqrt{\frac{D_m\left(1+\sqrt{7+\frac{3D_m}{x}}\right)}{2x+D_m}} \tag{5}$$

On the other hand, x, which determines the measure of width direction of models for calculation of elastic stiffness, is obtained by the following equation so that values of calculation of elastic stiffness are consistent with experimental and analytical results as described in the later chapter, where D is width of column, and B_f is width of the beam flange,

$$x = \alpha D\left(\frac{D}{B_f}\right)^{\beta}\left(\frac{D}{t_c}\right)^{\gamma} \tag{6}$$

$$\alpha = 0.60, \qquad \beta = 0.50, \qquad \gamma = -0.28 \qquad \text{(7.a)-(7.c)}$$

2.3 Yield Strength

Yield strength of the beam flange joint P_y is obtained by calculating force acting at the instant when exterior diaphragms at sections s_1, s_2, or s_3 shown in Fig.8 is yielded earliest. Sections s_1 - s_3 are located at positions where stress are relatively more higher than at other sections. We presume that wire elements at s_1 or s_2 are yielded by combining the bending moment and the shearing force, wire element at s_3 is yielded by combining the bending moment and the axial force, and the exterior diaphragm model shows elastic bevavior until the diaphragm yields at s_1 - s_3.

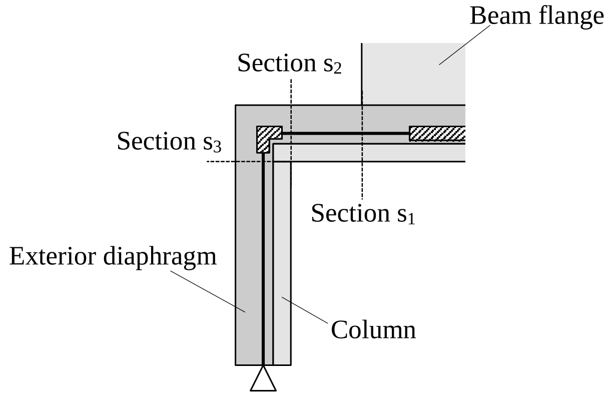

Fig.8 – Locations of examined sections

3. Verification of Validity of Evaluation Methods by Loading Tests and FEM Analysis

In this chapter, elasto-plastic behavior of beam flange joints has been investigated by loading tests and FEM analysis, and we compared calculated values with these results to verify the validity of evaluation methods.

3.1 Loading tests (T series)

3.1.1 Summary

The specimen of T series is shown in Fig.9. The area surrounded by a dotted line in Fig.9 corresponds to the beam flange joint, and the other area is the equipment for loading. Slits were designed for simulationg in-plane deformation of the exterior diaphragm of the tensile side in Fig.4(b). Both ends of the specimen were grabed with chucks of the tension tester, tensile force P were applied to specimen, and elasto-plastic behavior of beam flange joints was confirmed by static monotonous loading. δ was measured by the relative displacement between two dots shown in Fig.9. Summary of T series is shown in Table 1, where t_b is thickness of the beam flange, t_d and h_d are relatively thickness and depth of protrusion of the exterior diaphragm, ${}_c\sigma_y$, ${}_b\sigma_y$ and ${}_d\sigma_y$ are yield strength of the column, beam flange, diaphragm relatively. Material characteristic of steel is shown in Table 2. Details of column corner welds and fillet welds between each members are shown in Fig.10. These fillet welds were designed so that rupture of welds did not occar earlier than ruputure of base materials.

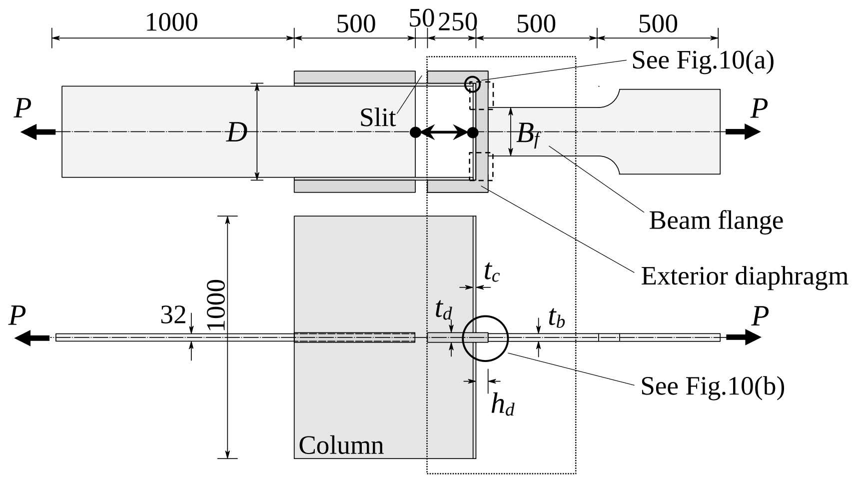

Fig.9 – Specimen of T, A and B series

Table 1 – Summary of T series

No.	Column				Beam flange				Exterior diaphragm				Elastic stiffness [kN/mm]			Yield strength [kN]		
	D [mm]	t_c [mm]	${}_c\sigma_y$ [N/mm^2]	Grade of steel	B_f [mm]	t_b [mm]	${}_b\sigma_y$ [N/mm^2]	Grade of steel	t_d [mm]	h_d [mm]	${}_d\sigma_y$ [N/mm^2]	Grade of steel	K_{cal}	K_{exp}	$\frac{K_{cal}}{K_{exp}}$	${}_{cal}P_y$	${}_{exp}P_y$	$\frac{{}_{cal}P_y}{{}_{exp}P_y}$
T1	400	12	811	H-SA700	200	32	581	SM570	40	50	442	550Mpa class steel	550	522	1.05	596	989	0.60
T2	500	25	867		300					45			932	911	1.02	1443	2016	0.72

Table 2 – Material characteristic of steel

Grade of Steel	Thickness [mm]	Part	Yield stress [N/mm^2]	Tensile strength [N/mm^2]	Yield ratio [%]
H-SA700	12	Column (T1)	811	851	95.3
	25	Column (T2)	867	907	95.6
550Mpa Class steel	40	Diaphragm	442	596	74.2
SM570	32	Beam flange	581	673	86.3

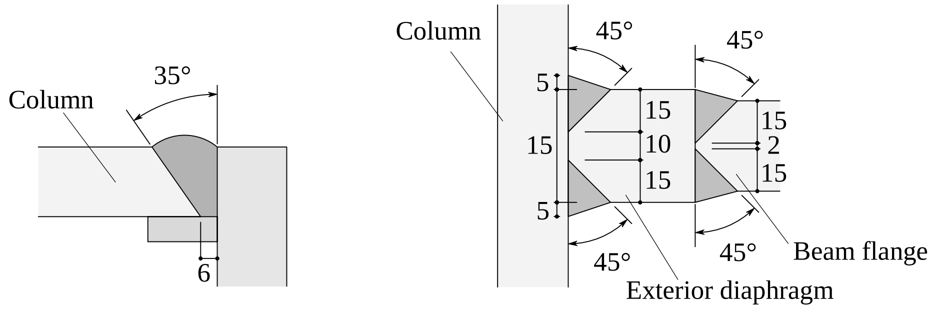

(a) Column corner welds (b) Fillet welds

Fig.10 – Details of welds (measure unit: mm)

3.1.2 Results of loading tests

Load deformation relationships of loading tests are shown with solid lines in Fig.11, and photos of T1 after loading are shown in Fig.12. Crack of column corner welds of both specimen occurred at points of rhombuses shown in Fig.11, and cracking reduced load. Furthermore, shear deformation of the exterior diaphragm surrounded by broken lines in Fig.11 occurred clearly at final time.

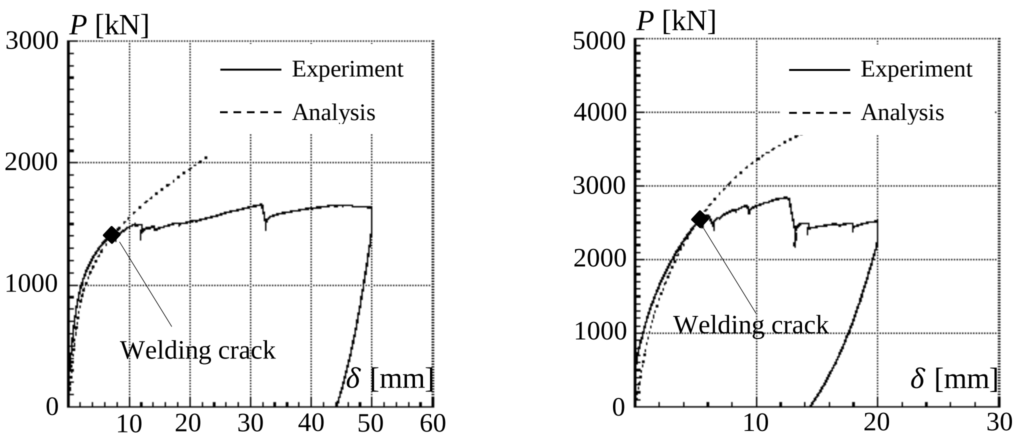

(a) T1 (b) T2

Fig.11 – Load deformation relationship of T series

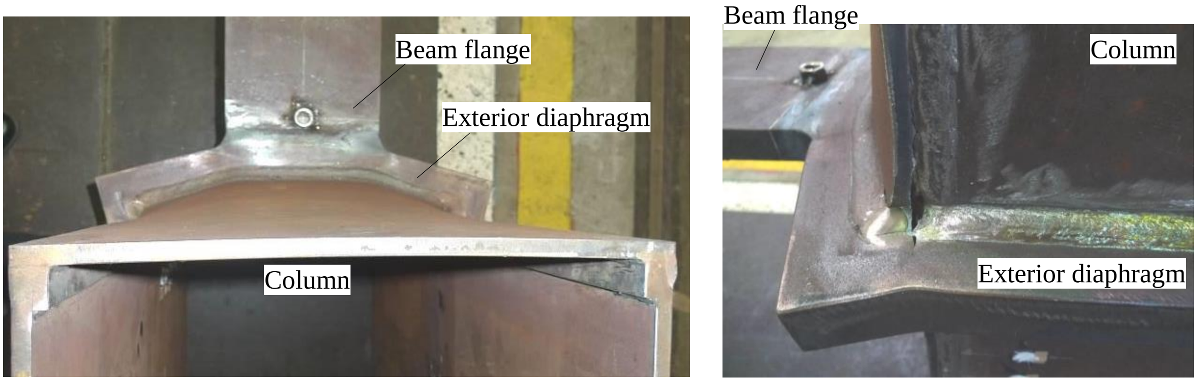

(a) Deformation of column and exterior diaphragm (b)Cracking of column corner welds

Fig.12 – Photos of T1 after loading

3.2 FEM analysis

3.2.1 Summary of FEM models of T series, and A and B series

To compare the elasto-plastic behavior of local tensile models of experiment and analysis, FEM analysis were conducted with models having same shapes shown in Fig.9. Furthermore, analysis A and B series were conducted to investigate elastic stiffness and yield strength of the beam flange joints of each analytical parameters.

ADINA was used about T and A series, and Abaqus was used about B series. Shapes of analysis A and B series were similar to Fig.9. Considering symmetry of model shapes, we used the quarter part of models with 8-node hexahedral solid elements. Yield condition was based on the von Mises yield condition, and isotropic hardening low was adapted.

Summary of A and B series is shown in Table 3. Analytical parameters of A and B series were thickness and width of columns, width of beam flanges, thickness and depth of protrusion of exterior diaphragms, and grade of steels and yield strength of each members. Considering actual sizes, width of columns was 800 -1000 mm in B series. Furthermore, beam flanges were treated as elastic body to focus on only plastic deformation of columns and exterior diaphragms.

Material properties of T series was defined by Table 2, and material properties of A and B series were defined by true stress ture strain relationship shown in Fig.13. Regarding material properties of beam flanges and diaphragms of A22 and A23, only yield strength were varied relatively while tensile strength was equal to strength of other models of A series. Deformation of the beam flange joint δ was obtained by the relative displacement between two dots shown in Fig.14.

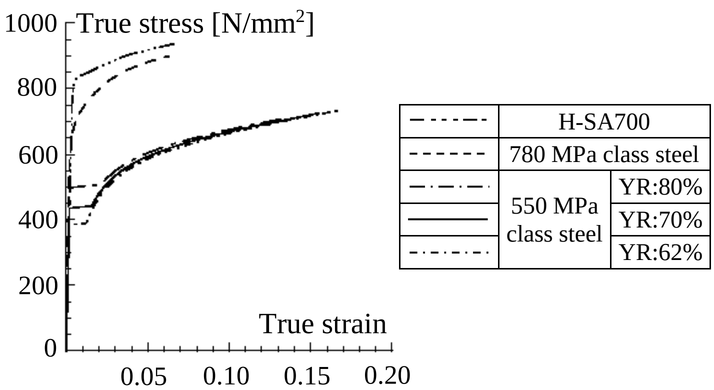

Fig.13 – True stress true - strain relationship

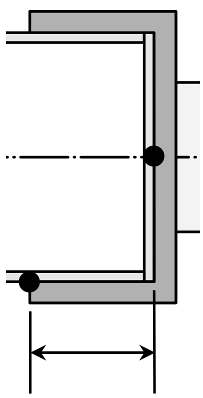

Fig.14 – Output points

Table 3 – Summary of FEM analysis

No.	Column				Beam flange				Exterior diaphragm				Elastic stiffness [kN/mm]			Yield strength [kN]		
	D [mm]	t_c [mm]	${}_c\sigma_y$ [N/mm²]	Grade of steel	B [mm]	t_b [mm]	${}_b\sigma_y$ [N/mm²]	Grade of steel	t_d [mm]	h_d [mm]	${}_d\sigma_y$ [N/mm²]	Grade of steel	K_{cal}	K_{FEM}	$\frac{K_{cal}}{K_{FEM}}$	${}_{cal}P_y$	${}_{FEM}P_y$	$\frac{{}_{cal}P_y}{{}_{FEM}P_y}$
A3			497	550Mpa class steel					45				985	968	1.02	1714	1933	0.89
A4										45			985	968	1.02	1714	2249	0.76
A5									36				890	904	0.98	1549	2022	0.77
A6	500								40				932	934	1.00	1622	2103	0.77
A7		25			300				50				1037	1000	1.04	1805	2338	0.77
A8										50			1063	1037	1.03	1773	2296	0.77
A9										60			1233	1165	1.06	1918	2432	0.79
A10										40			911	905	1.01	1664	2195	0.76
A11							497			36	497		857	850	1.01	1633	2110	0.77
A12	700					32		550Mpa class steel				550Mpa class steel	383	364	1.05	1103	1693	0.65
A13		19	824	H-SA700									264	257	1.03	659	1051	0.63
A14					250								789	770	1.02	1534	1997	0.77
A15		25			375				45				1357	1385	0.98	2042	2662	0.77
A16					425								1692	1728	0.98	2334	3035	0.77
A17					500					45			2248	2245	1.00	2803	3894	0.72
A18	500	12											463	477	0.97	692	1061	0.65
A19		19											674	718	0.94	1159	1549	0.75
A20		28			300								1190	1110	1.07	2078	2630	0.79
A21		32											1522	1313	1.16	2663	3268	0.81
A22		25					435				435		985	969	1.02	1500	2047	0.73
A23							385				385		985	969	1.02	1327	1917	0.69
B24									50				614	603	1.02	3329	6040	0.55
B25					300				45				602	583	1.03	3261	5924	0.55
B26		50							40	50			589	570	1.03	3193	5736	0.56
B27			824	H-SA700	200								424	499	0.85	3013	5371	0.56
B28	1000				400								821	737	1.11	3577	6669	0.54
B29										75			714	791	0.90	3306	5691	0.58
B30		40				32	Elastic body				497	550Mpa class steel	380	412	0.92	1987	4117	0.48
B31		50	675	780Mpa class steel	300				50				614	605	1.01	3331	5061	0.66
B32			824	H-SA700						50			1117	1091	1.02	4024	6310	0.64
B33	800	40											695	706	0.98	2427	4328	0.56
B34			675	780Mpa class steel									694	729	0.95	2433	3366	0.66
C35					400	32	Elastic body						891	869	1.03	4299	6623	0.65
C36													891	866	1.03	4299	5823	0.74
C37					300								669	727	0.92	3852	5523	0.70
C38	1000				400								891	898	0.99	4299	6062	0.71
C39		50			500								1139	1152	0.99	4793	6162	0.78
C40					600								1429	1528	0.94	5359	6237	0.86
C41					700								1783	2114	0.84	6034	6509	0.93
C42					400								1680	1763	0.95	5184	6182	0.84
C43	800				600					75			2906	3353	0.87	6927	6730	1.03
C44		40	824	H-SA700	400								1103	1239	0.89	3372	4256	0.79
C45					600								1900	2560	0.74	4506	5124	0.88
C46	700												2480	2672	0.93	5919	6460	0.92
C47	1200	50			400								537	528	1.02	3703	6055	0.61
C48					600	40	497	550Mpa class steel	50		497	550Mpa class steel	828	814	1.02	4544	6249	0.73
C49		40			400								580	621	0.93	2667	3934	0.68
C50					600								931	1103	0.84	3488	4333	0.80
C51	1000	60			400								1319	1272	1.04	6369	8253	0.77
C52										100			1031	1136	0.91	4364	5791	0.75
C53		50			600								1636	1859	0.88	5458	6214	0.88
C54										125			1197	1405	0.85	4600	5690	0.81
C55	800	40	675	780Mpa class steel	400								1103	1226	0.90	3372	3991	0.84
C56			497	550Mpa class steel						75			1103	1223	0.90	3372	3650	0.92
C57	1000	50	824	H-SA700	800								2235	2893	0.77	6888	6933	0.99
C58	800												4777	6392	0.75	9480	8611	1.10

3.2.2 Summary of C series

To simulate deformation of both tensile and compressive sides of the connection in Fig.4, analysis C series was conducted with models shown in Fig.15. Abaqus was used about C series. Supporting conditions at the top and bottom ends of the column was pinned support, and tensile or compressive force P were applied on both side beam flanges in the same direction. Considering actual sizes, width of columns was 700 - 1200 mm in c series. Analytical parameters was similar to A and B series. Material properties of C series was defined by Fig.13. Comparison with load deformation relationships of the entire model shown in Fig.15 and the local model shown in Fig.9 was shown in Fig.16. This figure shows that load deformation relationship of the entire model was consist with load deformation relationship of the local model, on condition that each members of these models have same measure.

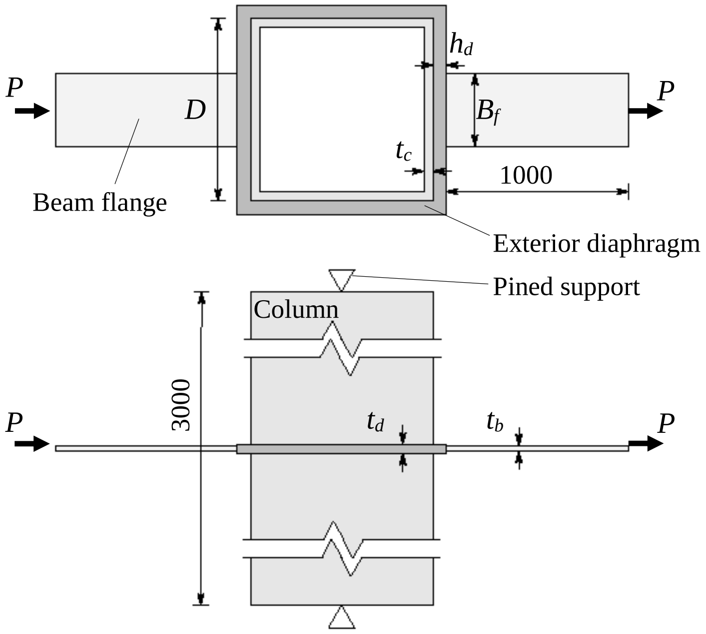

Fig.15 – Shapes of C series

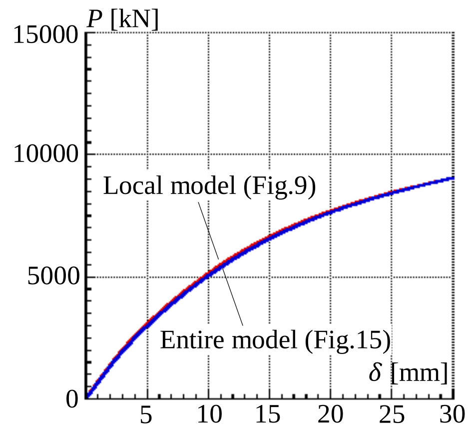

Fig.16 – Comparison with local model and entire model

3.2.3 Comparison with experimental and analytical results

Load deformation relationship of experiment and FEM analysis of T series is shown in Fig.11 to compare with these results. These graphs show P on the vertical axis and δ on the horizontal axis, solid lines represent experimental results, and dotted lines represent analytical results. These figures show good agreement between experimental results and analytical results from the initial state to the instant of cracking of column corner welds at loading tests. Especially, FEM analysis is able to simulate elastic stiffness and yield strength of beam flange joints of experiment except for the behavior after the crack.

3.3 Comparison with calculated values of elastic stiffness and yield strength and results of tests and FEM analysis

Comparison along calculated values of elastic stiffness and yield strength and experimental and analytical results is shown in Fig.17. These graphs show ratios of calculated values to experimental results or analytical results on the vertical axis, and the number of specimen (T series) and models (A, B, C series) on the horizontal axis. Fig.17(a) shows that calculated values of elastic stiffness are able to evaluate experimental and analytical results by 0 – 26 %. Fig.17(b) shows that, regarding T and A series, calculated values of yield strength are smaller than results of specimen and models having large width of the column or small thickness of the column by about 30 – 40%, and calculated values evaluate results of other specimen and models by about 10 – 30 %. As regard B series, Calculated values of yield strength are smaller than analytical results by about 30 – 50% because width of columns of B series are larger than width of beam flanges. Furthermore, with regard to C series, correspondence between calculated values of yield strength and analytical results is similar to A series, and calculated values of models whose width of beam flanges are larger than other models evaluate analytical results by about 0 – 20%.

●	T series
○	A series
△	B series
□	C series

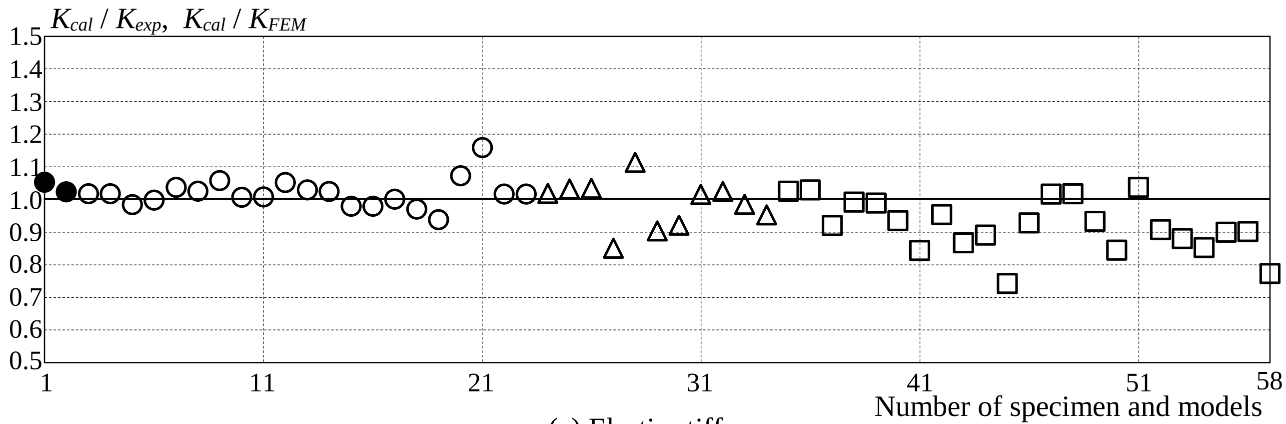

(a) Elastic stiffness

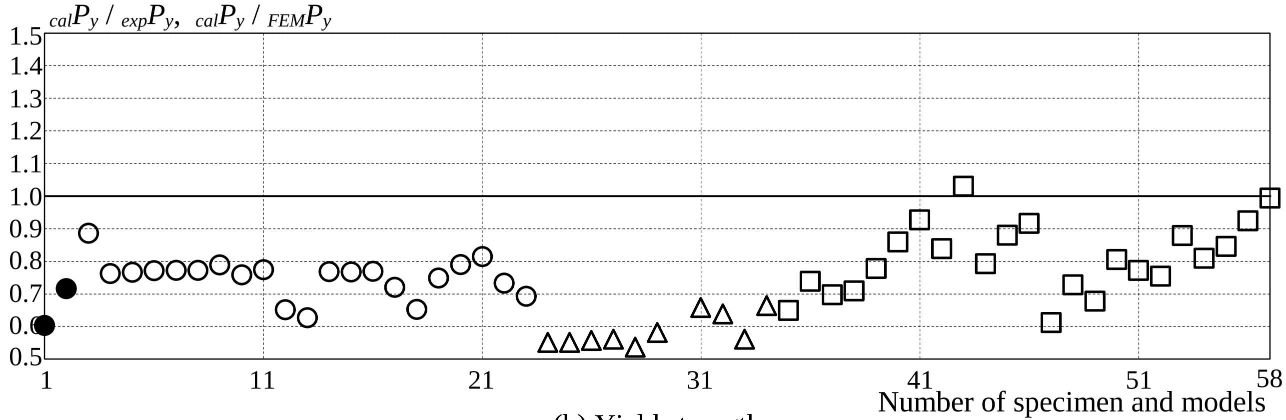

(b) Yield strength

Fig.17 – Comparison with calculated values and results of tests and FEM analysis

3.4 Correspondence with calculated values and load deformation relationship

Correspondence with calculated values of elastic stiffness and yield strength and load deformation relationship of C series is shown in Fig.18. Dotted lines represent calculated values of elastic stiffness, black-dots represent calculated values of yield strength, and outline dots represent analytical results of yield strength. These figures show good agreement between calculated values of elastic stiffness and initial stiffness of load deformation relationship. Although calculated values of yield strength are relatively lower than analytical results, calculated values of yield strength correspond to the instant when tangential stiffness slightly decline from initial stiffness. Therefore, it is assumed that this evaluation method of yield strength is appropriate as the evaluation method of strength of the elastic limit.

-------	Elastic stiffness	calculation
●	Yield strength	calculation
○	Yield strength	Analysis

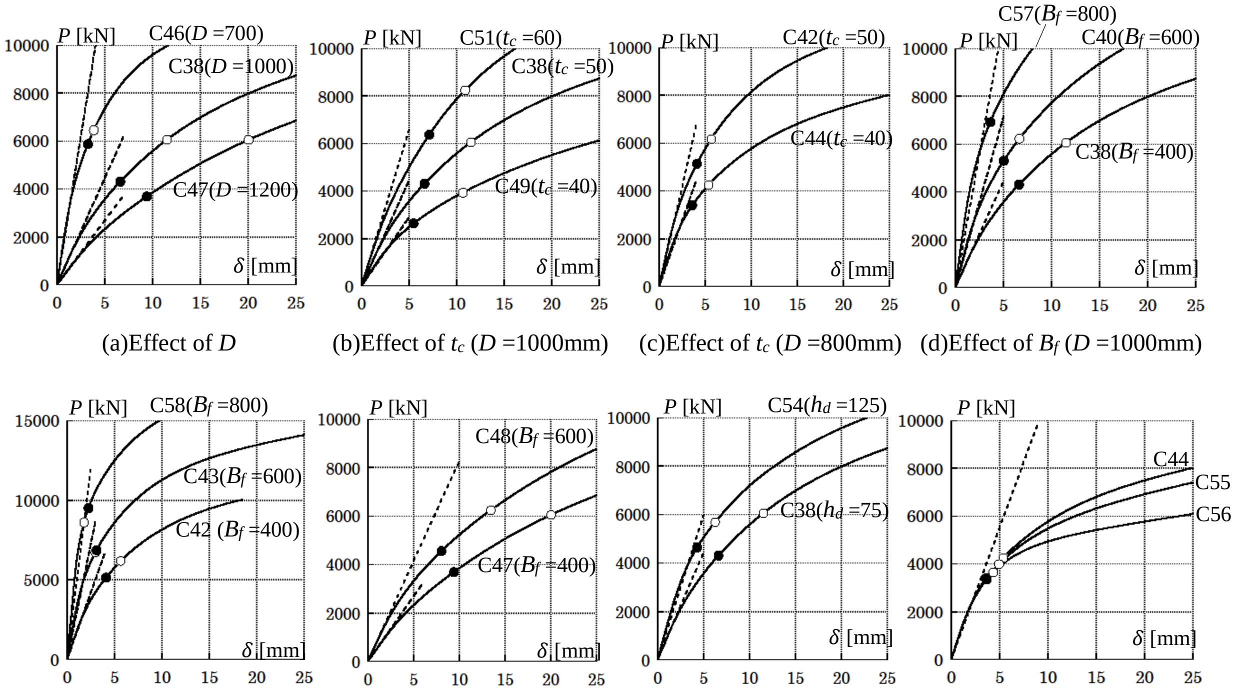

(a)Effect of D (b)Effect of t_c (D =1000mm) (c)Effect of t_c (D =800mm) (d)Effect of B_f (D =1000mm)

(e)Effect of B_f (D =800mm) (f)Effect of B_f (D =1200mm) (g)Effect of h_d (h)Effect of grade of column material

Fig.18 – Load deformation relationship of C series

4. Conclusion

This study regarded the square diaphragm of thick steel plates, whose depth of the protrusion is smaller than conventional exterior diaphragms. To evaluate elastic stiffness and yield strength of high strength steel box-shaped column to the beam flange joint in the exterior diaphragm moment connecton, we proposed two mechanical models, the exterior diaphragm model and the column model. To verify the validity of evaluation methods, we compared caluculated values with results of FEM analysis and tests, and obtained the following findings.

[1] Calculated values of elastic stiffness are able to evaluate experimental and analytical results by 0 – 26 %.

[2] Calculated values of yield strength evaluate results of many specimen and models by about 10 – 30 %, and correspond to the instant when the tangential stiffness slightly declined from the initial stiffness, and it is assumed that this evaluation method of yield strength was appropriate as the evaluation method of the elastic limit strength.

5. References

[1] Development of New Building Systems Using Innovative Structural Materials, JSSC, No.**75**, 2009, (in Japanese).

[2] The Japan iron and Steel Federation: Standard and Summary of Welding Construction of 780N/mm^2 Class High Strength Steel (H-SA700) for Architectural Structures, 2012, (in Japanese).

[3] Nakamura, Y., Matsuo, A., Kammaki, H.: An Experimental Study on Elasto–Plastic Behavior of Ring-type Exterior Diaphragm of RHS Column-to-H Beam Connections, Steel Construction Engineering, Vol.5, No.20, pp.45-52, December 1998

[4] Ito, A., Tanaka, T., Tabuchi, M., Yamaguchi, A., Matsushita, M.: Strength of SHS Column to Beam Connections Stiffened by Exterior Ring Diaphragms, J. Struct. Constr. Eng., AIJ, Vol.76, No.668, pp.1855-1864, Oct. 2011

[5] Kawai, T., Kondo, K.: Collapse Load Analysis of Bending Plates by a New Discrete Model, The Society of Naval Architects of Japan, No.142, pp.190-196, December 1977